Available online at www.sciencedirect.com
SCIENCE DIRECT®
International Journal of Heat and Fluid Flow 26 (2005) 771–779
International Journal of HEAT AND FLUID FLOW
www.elsevier.com/locate/ijhff

# Turbulent junction flow with an upstream ribbed surface

Khalil A. Kairouz [1], Hamid R. Rahai *

*Center for Energy and Environmental, Research and Services (CEERS), Department of Mechanical and Aerospace Engineering, California State University, Long Beach, CA 90840, United States*

Received 6 August 2004; accepted 1 February 2005
Available online 7 April 2005

**Abstract**

Results of experimental investigations of the effects of an upstream longitudinal triangular ribbed surface on a turbulent junction flow and downstream wake are presented. The ribbed plate was placed right upstream of the wing on the flat plate surface, covering a $10 \times 38$ cm$^2$ area. The junction flow was developed using a NACA0012 airfoil mounted normal to a flat plate downstream of its leading edge. The experiments were carried out at a free stream mean velocity of 31 m/s. which corresponds to a unit Reynolds number of $1.8 \times 10^6$ and the airfoil chord length Reynolds number of $5.4 \times 10^5$. Measurements were carried out at four control planes of 50%, 100%, 133%, and 166% of the wing chord length. Results show that the riblets displace the location of the horseshoe vortex away from the corner and reduce its strength. There are significant reductions in mean streamwise circulation downstream at 133% and 166% planes.


## 1. Introduction

The presence of adverse pressure gradients upstream of the wing in a wing–body junction results in flow separation upstream of the wing leading edge and generation of a separation line on the flat surface around and downstream of the wing. The existence of this separation line causes the skew induced streamwise vorticity to wrap around the nose of the wing with its leg trailing downstream in the corner between the wing–wake and the boundary layer. The effect of this structure, which is known as the horseshoe vortex is to bring high momentum free stream fluid toward the corner, which results in high surface shear stress, and larger drag and heat transfer rate.

The vortex size and strength changes with the nose bluntness factor as described by Mehta (1984), and Rood (1984), and a correlation presented by Fleming et al. (1993). The bluntness factor, BF, is defines as

$$\mathrm{BF} = \frac{1}{2}\frac{R_0}{X_T}\left[\frac{T}{S_T} + \frac{S_T}{X_T}\right]$$

Here $R_0$ is the leading-edge radius, $T$ and $X_T$ are, respectively, the maximum thickness and its corresponding chorwise position, and $S_T$ is the distance from the leading edge along the airfoil surface to the maximum thickness. For large bluntness factors, a bimodal structure exists for the velocity components around the front of the wing at the location where the flow is accelerating. This structure is perpendicular to the core of the horseshoe vortex and results in increased turbulent shear stress and kinetic energy within and beneath the vortex (Devenport and Simpson, 1990, 1992; Ölcmen and Simpson, 1994). However, according to Ölcmen and Simpson (1994) no binomial structure was found for a junction flow with a NACA 0012 airfoil with a 0.037 bluntness factor.

Simpson (2001) provides extensive reviews of previous experimental and computational investigations of

* Corresponding author. Tel.: +1 562 985 4407; fax: +1 562 985 4408.
*E-mail address:* rahai@csulb.edu (H.R. Rahai).
[1] Present address: Engineering Manager, Carollo Engineers, Fountain Valley, CA, United States.

0142-727X/$ - see front matter © 2005 Elsevier Inc. All rights reserved.
doi:10.1016/j.ijheatfluidflow.2005.02.002

**Nomenclature**

| | |
|---|---|
| $A$ | area, $m^2$ |
| $L$ | axial distance, m |
| $y$ | vertical distance, m |
| $U$ | axial mean velocity, m/s |
| $V$ | vertical mean velocity, m/s |
| $W$ | transverse mean velocity, m/s |
| $u'$ | rms axial turbulent velocity, m/s |
| $v'$ | rms vertical turbulent velocity, m/s |
| $w'$ | rms transverse turbulent velocity, m/s |
| $\overline{uv}$ | primary turbulent shear stress, $m^2/s^2$ |
| $C_f$ | skin friction coefficient, $\frac{\tau_0}{\frac{1}{2}\rho U_\infty^2}$ |
| $D_J$ | junction drag force, N |
| $F_i$ | pressure force at control volume inlet, N |
| $F_e$ | pressure force at control volume outlet, N |
| $Re$ | Reynolds number, $\frac{U_\infty L}{\nu}$ |
| $\mu$ | dynamic viscosity, $\frac{N\,s}{m^2}$ |
| $\nu$ | kinematic viscosity, $m^2/s$ |
| $U_e$ | axial mean velocity at the edge of boundary layer, m/s |
| $U_\infty$ | free stream mean velocity, m/s |
| $V_n$ | normal mean velocity, m/s |
| $\rho$ | density, $kg/m^3$ |
| $\Omega_x$ | normalized vorticity in $x$ direction, $cm^{-1}$, $\frac{\partial(\frac{V}{U_e})}{\partial z} - \frac{\partial(\frac{W}{U_e})}{\partial y}$ |
| $\Gamma_x$ | circulation in $x$ direction, cm, $\int\int \left[\frac{\partial(\frac{V}{U_e})}{\partial z} - \frac{\partial(\frac{W}{U_e})}{\partial y}\right] dy\,dz$ |

the junction vortices and works related to control, modification, or elimination of such vortices. Relevant to the present study are investigations by Sung et al. (1988) and Kubendran et al. (1988) who studied the effects of large fairing placed between the nose of the wing and the flat plate surface on junction flow structure. Their results show that the large fairing reduces the strength of the vortex legs downstream and eliminates the leading edge flow separation. In addition, placing fillets between the base of the wing and the flat surface results in disappearance of low momentum fluid and reduction of the interference drag.

Devenport et al. (1990) studied the effects of a fillet with uniform radius wrapped around the entire base of the wing, on the leading edge flow separation and horseshoe vortex in an idealized wing–body junction. Their investigations show that the presence of the fillets results in displacement and not the elimination of the separation line and the location of the horseshoe vortex, similar to having a larger leading edge diameter.

Results of previous studies have shown that the presence of the flow separation line and generation of the skew induced vorticity upstream of the wing is due to the existence of spanwise pressure gradients on the flat plate surface upstream of the wing. Reduction or modifications of these pressure gradients should affect the separation line upstream and thus changes the structure and possibly the strength of the vortex leg downstream.

Longitudinal ribbed surfaces have been used as effective drag reduction devices. A comprehensive review of previous research on riblets is presented by Walsh (1990). The role of the riblets is to interact with the low speed regions within a turbulent boundary layer to constrain the growth of the low speed streaks and thus reduce the turbulence energy within the boundary layer which leads to reduction in the surface skin friction. Previous investigations have shown that for a V-groove riblet, effective reduction in the skin friction can be obtained with $h/s = 0.3$–$0.5$. Here $h$ and $s$ are the height and spacing of the riblet, respectively. The dimensionless $h$ and $s$ are defined as: $h^+ = hRe\sqrt{C_f/2}$, $s^+ = sRe\sqrt{C_f/2}$. Here $Re$ is the unit Reynolds number and $C_f$ is the local skin friction coefficient. When $h^+$ is higher than 60, for a dimensionless boundary layer thickness $y^+ < 15$ ($y^+ = yRe\sqrt{C_f/2}$), the riblets create a controlled spanwise mean velocity gradient with minimum velocity occurring over the valleys for a closely-spaced riblets and over the peaks for a widely spaced riblets. The spanwise mean velocity gradient is related to the spanwise pressure gradient. Thus, for a junction flow, it is possible to control the location of the upstream separation line and reduce the axial angle of the horseshoe vortex, using a ribbed surface.

## 2. Experimental procedure and techniques

The experiments were carried out in the open circuit boundary layer wind tunnel of the Center for Energy and Environmental Research and Services, CEERS, at CSULB. It is an open-circuit wind tunnel with a variable speed centrifugal fan, a wide angle diffuser, a settling chamber with flow conditioners, a 6:1 three-dimensional contraction connected to a test section and a wide angle exit diffuser. The test section has a constant rectangular cross section of $16.5 \times 38.1$ cm and is 208 cm long. The walls and floor are made of Plexiglas, and the top is made of plywood. The plywood top has streamwise and spanwise slots at various locations to allow insertion of a probe for data acquisition. For the present experiments, all sides were adjusted to compensate for the boundary layer growth when the wing was not in place.

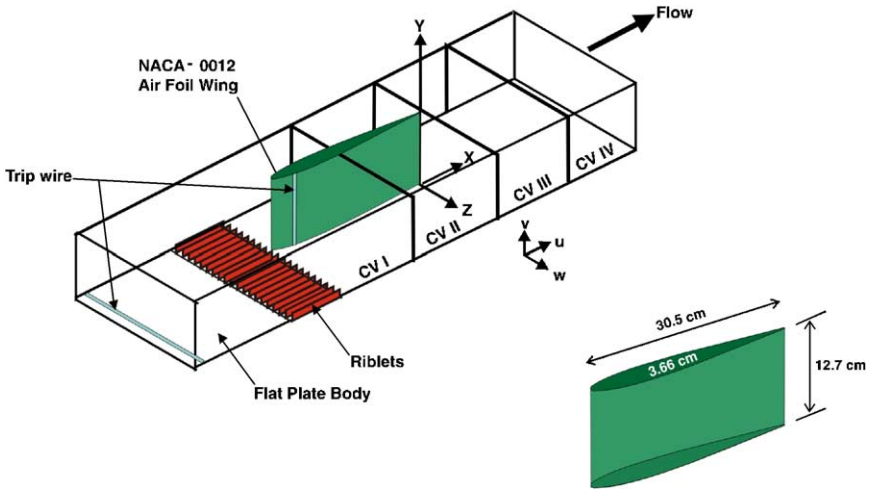


Fig. 1. Experimental set-up.

All experiments were carried out at an isothermal free stream mean velocity of 31 m/s which corresponds to an approximate unit Reynolds number of $1.8 \times 10^6$. The free stream turbulence intensity was less than 0.5%. The non-uniformity in the free stream mean velocity was less than 0.2% and in the free stream turbulence intensity was less than 1%.

The flow configuration for the present study is depicted in Fig. 1. The "body" is the bottom side of the wind tunnel test section which is made of a 1.6 cm thickness Plexiglas. The wing is an NACA-0012 airfoil which has a maximum thickness of 3.66 cm, a height of 12.7 cm, and a length of 30.5 cm and is placed 91.5 cm downstream of the body leading edge at zero angle of attack. Wires of 3 mm diameters are attached to the surfaces of the wing and the wind tunnel floor (the body) at 2.54 cm from their leading edges to ensure early transition of the boundary layers to turbulent.

Longitudinal triangular riblets were placed upstream of the wing on the tunnel floor. The length of the surface area covered by the riblets was 10 cm and spanned the width of the test section. The triangular riblet had a flute height of 0.168 cm and a flute spacing of 0.235 cm. These dimensions correspond to widely spaced riblets which should place the location of the minimum velocity over its peaks. The ratio of the flute height to the boundary layer thickness, $\frac{h}{\delta}$, measured at the leading edge of the riblets was approximately 0.1.

Mean flow characteristics were investigated using a specially made miniature five hole probe with a tip outside diameter of 1.7 mm and a length of 60 mm connected to five channels of a Validyne DP 15–48 differential pressure transducer. A cylindrical stainless steel cylinder with 4.8 mm O.D. attached perpendicular to the probe axis at its mid-length connected the probe to a traverse mechanism outside the wind tunnel. (Details of the probe and its calibration curves are given by Zagres (1997).) In addition, the wind tunnel throat velocity was obtained from pressure differential measurement using another channel of the Validyne unit. The outputs of the transducers were connected to six channels of Metrabyte DAS-20 A/D board, connected to a Pentium based micro processor. Measurements were carried out at four planes perpendicular to the axial flow direction. The planes were at 50%, 100%, 133% and 166% of the wing chord length. These planes were identified as CVI-CVIV. At each plane more than 15 profiles were obtained and analyzed.

Measurements were made on one side of the wing–body junction and downstream, due to the flow symmetry, both with and without the riblets in place.

Turbulent junction flow as well as the downstream interaction regions between the wing–wake and flat plate boundary layer were investigated using a TSI X hot wire probe model 1243 in conjunction with two channels of IFA 100 Intelligent flow analyzer. Measurements were carried out at the same locations where the mean flow characteristics were investigated. For each location 50 records per channel where each record contains 2048 samples of data were digitized at a sample rate of 6000 samples/s, using two channels of DAS-20 Analog to digital converter connected to a Pentium based micro-computer. Results were analyzed using standard software supplied by Data Ready, Inc.

## 3. Results and discussions

Fig. 2 shows normalized streamwise mean velocity contours, the secondary flow vector, and the contours of normalized axial and vertical turbulent velocities and primary turbulent shear stress at CVI plane, with and without the riblets in place. Results with the riblets show reductions in the secondary velocity and mean

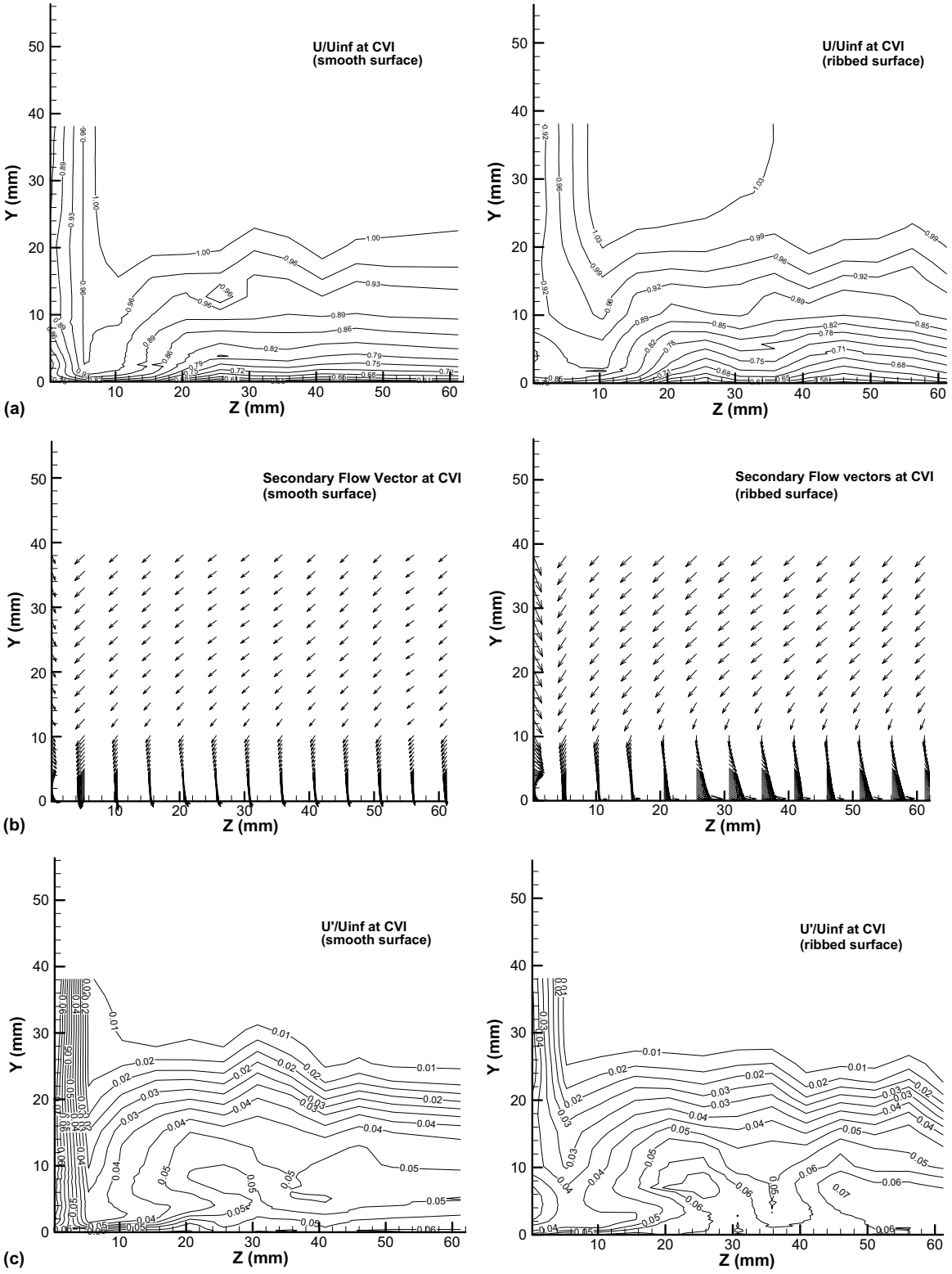


Fig. 2. Contours of normalized: (a) axial mean velocity; (b) secondary flow vector; (c) axial turbulent velocity; (d) vertical turbulent velocity and (e) primary turbulent shear stress at CVI.

velocity gradient near the flat plate surface. At $Z = 5.1$ mm, there is considerable reduction in the secondary velocity and for $Z < 20$ mm, the acceleration of the flow toward the corner is reduced which are indications of a weaker secondary flow. For $Z > 20$ mm, near the flat plate surface, there is a change in the direction of

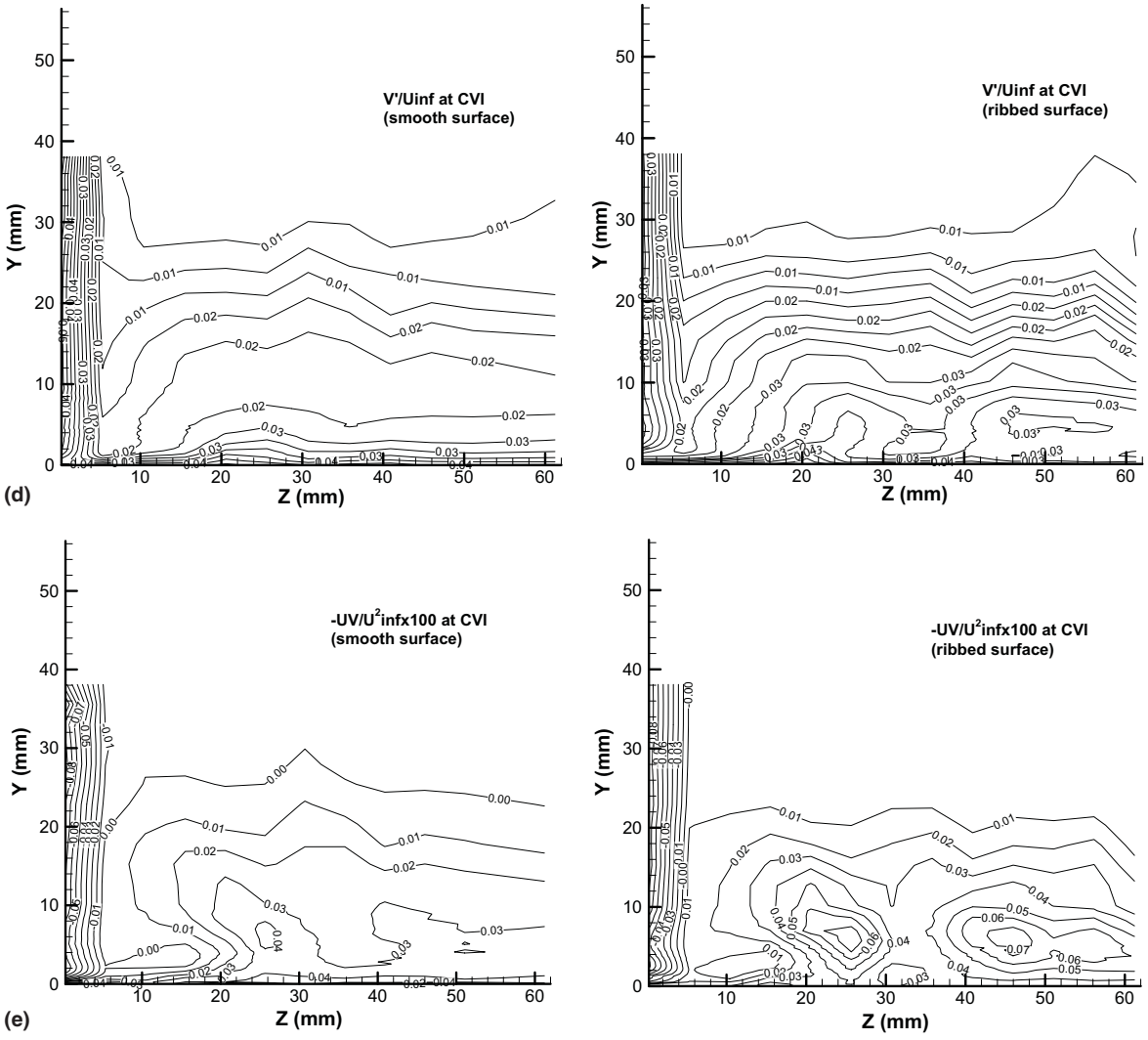


Fig. 2 (*continued*)

the secondary flow with flow moving toward the edge of the flat plate boundary layer. For $Y > 5$ mm, the secondary flow has lost its momentum considerably.

The axial and vertical turbulent velocities and turbulent shear stress show increases near the flat plate surface for $Z > 20$ mm. These are the areas where the displaced horseshoe vortex has moved, resulting in increased Reynolds stresses.

Fig. 3 shows similar results as shown in Fig. 2 at CVII plane. When the riblets are not in place, the isovel contours show steep velocity gradient near the flat plate surface near the wing trailing edge, while the corresponding results with the riblets show reduced velocity gradient at these locations. There is an increase in the secondary flow toward the corner as compared to the corresponding results for CVI with the riblet in place. However, there are still noticeable reductions in the secondary flow near the flat plate surface for $10\text{ mm} < Z < 20$ mm, when compared with the corresponding results without the riblets in place.

As in CVI, the riblets have weakened and displaced the horseshoe vortex toward the edge of the flat plate, resulting in slight increases in the axial and vertical turbulent velocities and turbulent shear stress at these locations.

Results at the CVIII and CVIV planes (not presented here) show that the effects of the riblets on the horseshoe vortex and turbulent stresses have reduced considerably. The presence of the wing wake has further moved the horseshoe vortex away from the bisecting plane and toward the edge of the flat plate.

The added drag due to the secondary flow kinetic energy in a wing–body junction configuration can be calculated from the following equation as:

$$D_a = Q \int \frac{V^2 + W^2}{U_\infty^2} \mathrm{d}A$$

At CVI plane the added drag with and without the riblets are respectively, 0.0065 and 0.013 N and at CVII plane, these values are respectively, 0.0063 and 0.024 N.

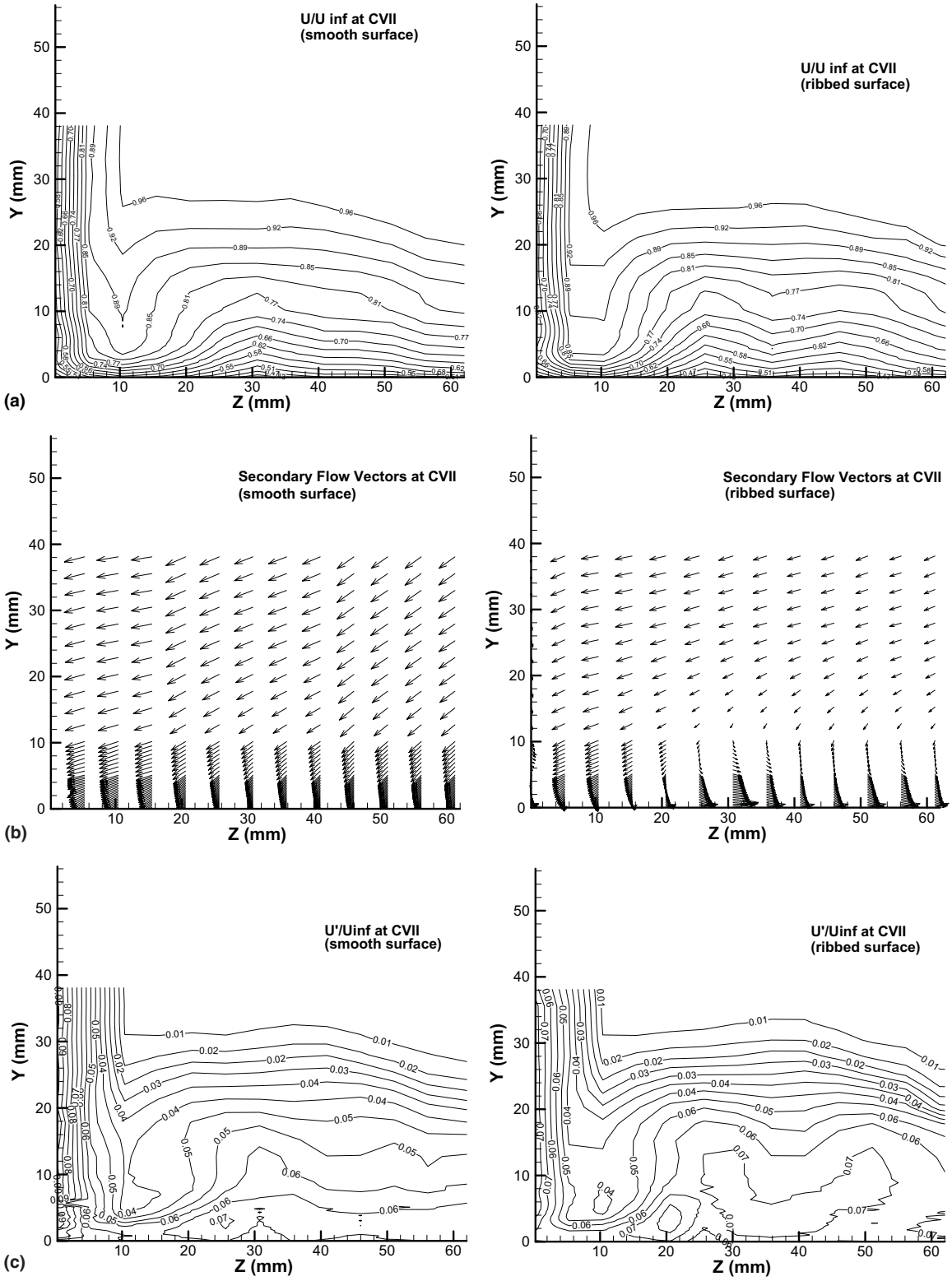


Fig. 3. Contours of normalized: (a) axial mean velocity; (b) secondary flow vector; (c) axial turbulent velocity; (d) vertical turbulent velocity and (e) primary turbulent shear stress at CVII.

These results indicate that placing the riblets within the boundary layer upstream of the wing, in a junction flow configuration can reduce the strength of the secondary flow considerably.

Fig. 4 shows mean streamwise vorticity contours at CVI and CVII. For $y < 4$ mm, there are increased vorticity when the riblets are in place and with slight reductions in the vorticity at the corner. The riblets are

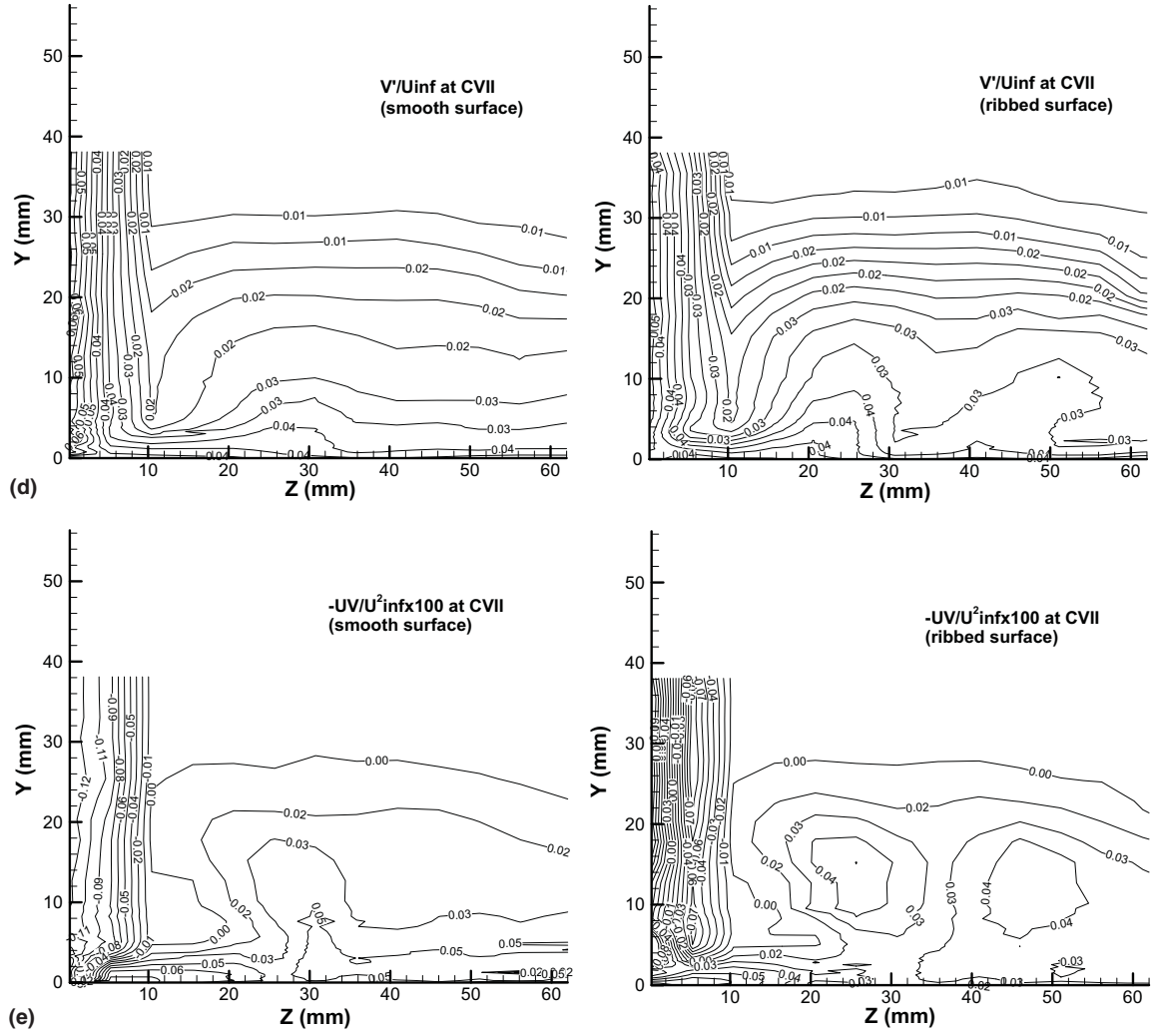


Fig. 3 (*continued*)

acting as thin axial fins along the flat plate, with increased vorticity between the fins and in the wake, but limiting these vorticity very close to the flat plate surface. There are reductions in the vorticity at the corner near the flat plate surface at CVI and CVII planes. Results at CVIII and CVIV planes (not shown here) show less reductions in vorticity away from the wing–wake flat plate boundary layer interaction regions.

The circulation obtained from integration of the streamwise vorticies at the four planes are, respectively, 0.12, 0.041, 0.028, and 0.05 $m^2/s$ with the riblets in place and 0.15, 0.047, 0.047, and 0.1 $m^2/s$ without the riblets. The effects of the riblets are seen as reductions in the circulation in the corner and at the immediate downstream interaction regions.

Junction drag was calculated from a momentum balance for a control volume with CVIV plane with and without the riblets in place using the following equation:

$$D_J + F_i - F_e = \int \rho \cdot U \cdot V_n \cdot dA$$

The pressure forces at the inlet and exit of the control volume ($F_i$ and $F_e$) were nearly the same and thus their net contributions were taken as zero and with the momentum fluxes being zero on the solid surfaces, placing the upstream riblets results in about 2% increase in drag at CVIV. The ribelts have reduced the secondary flow momentum resulting in added axial momentum which has increased the junction drag. Even though there are some variations in pressure forces due to the wing–wake at the exits of the CVII and CVIII planes, however, increases in the junction drag are expected at these locations also.

The mechanical power losses for all four planes with and without the riblets in place were obtained by integrating over each plane area the product of normal velocity, free stream dynamic pressure and the total pressure coefficient. Results indicate that with the riblets in place, the power loss decreases by 22% and 18% at planes CVI and CVII and by 49% and 70% at planes CVIII and CVIV respectively. The decrease in the power losses is due to reduced secondary flow at these locations.

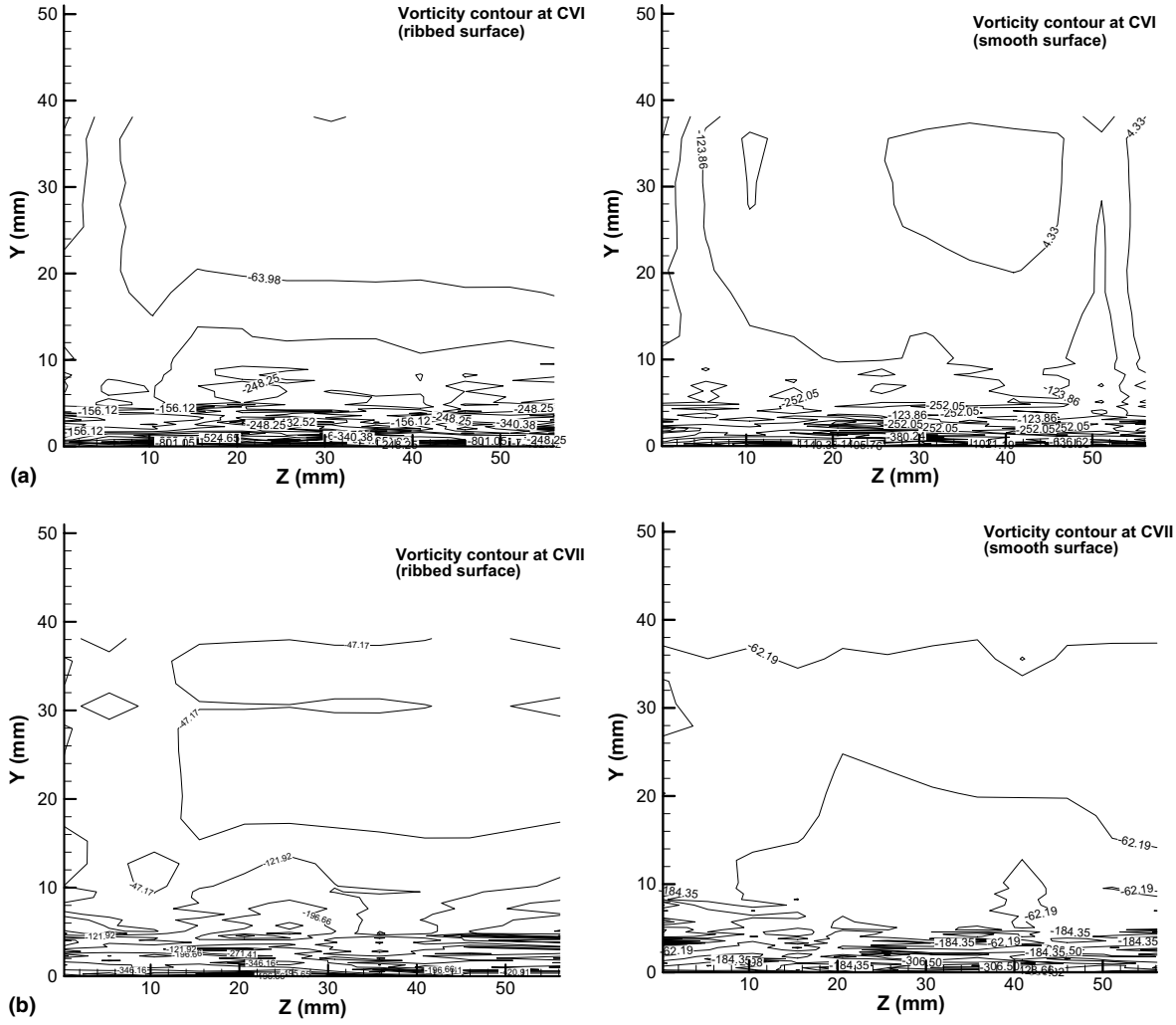


Fig. 4. Contours of normalized axial vorticity at: (a) CVI and (b) CVII.

## 4. Conclusions

The effects of placing riblets on a flat surface within a turbulent boundary layer upstream of an NACA 0012 airfoil which is placed perpendicular to the flat plate, on the junction flow and downstream wing–wake flat plate-boundary layer interaction regions were experimentally investigated. The experiments were carried out at four planes of 50%, 100%, 133%, and 166% of the airfoil chord length. Results indicate that the presence of the riblets result in reductions of the secondary flow and turbulent Reynolds stresses near the corner at 50% and 100% planes and away from the interaction regions at 133% and 166% planes. The reductions in the secondary flow were accompanied by reductions in the mean streamwise vortices.

There were reductions in the circulation at these planes with the riblets in place, resulting in reduced added secondary flow drag.

These results indicate that riblets may be a good passive controller in reducing the strength of the secondary flow in a junction configuration.

*Statement of uncertainty*. For all measurements, the uncertainty in normalized mean velocity is ±0.005 in turbulence intensities is ±0.02 turbulent shear stress is ±0.0004 and in $x/d$, $y/d$, and $z/d$ is ±0.05 at 20:1 odd.

## References

Devenport, W.J., Simpson, R.L., 1990. Time dependant and time-averaged turbulence structure near the nose of a wing–body junction. J. Fluid Mech. 210, 23–55.

Devenport, W.J., Simpson, R.L., 1992. Flow past a wing–body junction: experimental evaluation of turbulence models. AIAA J. 30, 873–881.

Devenport, W.J., Agarwal, N.K., Dewitz, M.B., Simpson, R.L., Poddar, K., 1990. Effects of fillets on flow past a wing–body junction. AIAA J. 28 (12), 2017–2024.

Fleming, J., Simpson, R.L., Devenport, W.J., 1993. An experimental study of a turbulent wing–body junction and wake flow. Exp. Fluids 14, 366–378.

Kubendran, L.R., Bar-Sever, A., Harvey, W.D., 1988. Flow control in a wing/fuselage type junction, AIAA Paper 88-0614.

Mehta, R.D., 1984. Effect of a wing nose shape on the flow in a wing/body junction. Aerosp. J. 88, 456–460.

Ölcmen, M.S., Simpson, R.L., 1994. Influence of wing shapes on surface pressure fluctuations at wing–body junction. AIAA J. 32, 6–15.

Rood, E.P., 1984. The governing influence of the nose radius on the unsteady effects of large scale flow structure in the turbulent wing and plate junction flow, ASME Forum on Unsteady Flow, ASME Fluids Engineering Division, New York, No. 15, pp. 7–9.

Simpson, R.L., 2001. Junction flows. Ann. Rev.—Fluid Mech. 33, 415–443.

Sung, C.-H., Yang, C.-I., Kubendran, L.R., 1988. Control of horseshoe vortex juncture flow using fillet, In: Proceedings of the Symposium on Hydrodynamic Performance Enhancement for Marine Applications, Newport, RI.

Walsh, M.J., 1990. "Riblets", in viscous drag eduction in boundary layers. Bushnell, D.M., Hefner, J.N., (Ed.), Progress in Astronautics and Aeronautics, Vol. 123, pp. 203–261.

Zagres, D., 1997. MS Thesis, Mechanical Engineering Department, California State University, Long Beach.